

Preliminary Study on the Effect of 4DCT-Ventilation-Weighted Dose on the Radiation Induced Pneumonia Probability (RIPP)

Dose-Response:
An International Journal
July-September 2021:1-7
© The Author(s) 2021
Article reuse guidelines:
sagepub.com/journals-permissions
DOI: 10.1177/15593258211017753
journals.sagepub.com/home/dos



Han Bai^{1,2} , Wenhui Li¹, Yaoxiong Xia¹, Lan Li¹, Jingyan Gao¹, and Xuhong Liu¹

Abstract

Purpose: The purpose of the present study was to evaluate the feasibility of using 4-dimensional computed tomography (4DCT)-ventilation-weighted dose analysis to predict radiation-induced pneumonia probability (RIPP).

Methods and Materials: The study population for this retrospective analysis included 16 patients with stage III lung cancer. Each patient's 4DCT images, including end-inhale and end-exhale sequences, were used for the deformable image registration, and the Hounsfield units (HU) density-change was used to calculate the ventilation. A previously established equation was used to convert the original dose (OD) $D_{0,i}$ in the lungs in the original plan (OP) to the weighted-dose (WD) $D_{w,i}$ in the weighted plan (WP). The patients were divided into 2 groups, one with radiation-induced pneumonia (RIP), and one without. The Spearman correlation analysis was used to analyze the correlation of RIP with ΔV_{20} ($\Delta V_x = V_{w,x}$ in the WP – $V_{0,x}$ in the OP), Δ MLD (Δ MLD = mean lung dose (MLD) in the WP – MLD in the OP), and ΔV_5 .

Results: The results showed that 5 of the 16 patients were suffering from acute RIP, 4 of which had higher ΔV_{20} and Δ MLD values than the rest of the patients. The results of the Spearman correlation analysis for those 4 patients were as follows: RIP vs. ΔV_{20} , $r = 0.5123$; RIP vs. Δ MLD, $r = 0.5119$; RIP vs. ΔV_5 , $r = 0.1904$.

Conclusions: The 4DCT-ventilation-based weighted-dose analysis showed some correlation between RIPP and both ΔV_{20} and Δ MLD, when comparing the weighted-dose and the conventional dose-volume histogram (DVH) analyses.

Keywords

4DCT-ventilation, weighted dose, original dose, ventilation change, radiation-induced pneumonia

Introduction

Radiotherapy plays an important role in the comprehensive treatment of lung cancer. Hypofractionated radiotherapy is the best treatment for stage I-II ($T_{1-3}N_0-T_{1-2}N_1$) lung cancer patients, especially for elderly patients with comorbidities who are not ideal candidates for surgery. Previous studies have shown that stereotactic body radiation therapy (SBRT) results in fewer complications, but has almost the same local control rate as surgery.^{1,2} Concurrent chemoradiotherapy is recommended for locally advanced stage II-III lung cancer, while radiotherapy is considered a local consolidation therapy for stage IV lung cancer metastases.³

The tolerance dose of lung tissue is still the primary constraint for improving the target dose. The radiation dose to the lung tissue has continuously decreased with the growth and development of treatments and technology. One report has demonstrated that symptomatic radiation-induced pneumonia

(RIP) and fibrosis were serious complications occurring in an estimated 5-50% of patients with lung cancer.⁴ The effect of the continuous improvement of radiotherapy techniques to further reduce the dose to the lung is decreasing. In this regard, functional lung avoidance radiotherapy has been proposed.^{5,6} In this process, the lung is first divided into a high functional area

¹ Department of Radiation Oncology, The Third Affiliated Hospital of Kunming Medical University, Yunnan Tumor Hospital, Kunming, Yunnan, China

² Department of Physics and Astronomy, Yunnan University, Kunming, Yunnan, China

Received 8 June 2020; received revised 2 April 2021; accepted 7 April 2021

Corresponding Author:

Wenhui Li, Department of Radiation Oncology, Tumor Hospital of Yunnan Province, No.519 Kunzhou Road, Xishan District, Kunming 650118, China.
Email: bh001925@163.com



Creative Commons Non Commercial CC BY-NC: This article is distributed under the terms of the Creative Commons Attribution-NonCommercial 4.0 License (<https://creativecommons.org/licenses/by-nc/4.0/>) which permits non-commercial use, reproduction and distribution of the work without further permission provided the original work is attributed as specified on the SAGE and Open Access pages (<https://us.sagepub.com/en-us/nam/open-access-at-sage>).

(HFA) and a low functional area (LFA), based on functional imaging results. Then, the radiotherapy planning is designed to spare as much of the HFA as possible, based on the subarea, as one opinion suggested that sparing the HFA may reduce the occurrence of pulmonary complications.

Functional avoidance based on positron emission tomography (PET),⁷ single-photon emission computed tomography (SPECT),⁸ magnetic resonance imaging (MRI),⁹ and 4-dimensional computed tomography (4DCT)-ventilation¹⁰⁻¹² imaging has been demonstrated in a variety of studies. Of these methods, 4DCT-ventilation imaging, which uses data to create lung function maps for functional avoidance planning, is the most ideal. Compared with other imaging modalities, 4DCT-ventilation imaging provides functional information from standard treatment procedures without additional image acquisition, which does not increase the economic burden on the patient. Furthermore, 4DCT-ventilation imaging allows for rapid image processing without the need for a radioactive contrast agent, and provides a 4-D map of anatomical structures.

The history of development of 4DCT-ventilation for functional lung avoidance radiotherapy can be found in retrospective studies by institutions worldwide.¹¹⁻¹³ However, previous studies involving 4DCT-ventilation imaging for functional lung avoidance have primarily focused on demonstrating the feasibility of sparing HFAs. Little information in current literature addresses the evaluation of dose-volume in relation to functional weight, because planning the avoidance of HFAs would inevitably increase the dose to LFAs. The acquisition of data regarding functional avoidance and loss of functional defect are expected to be obtained. The first goal of data acquisition is to evaluate the ratio of the functional area to the functional defect area. Since the HFA has a higher ventilation capacity and oxygen concentration than the LFA, and oxygen is known to increase tissue sensitization to radiation therapy, the Hounsfield unit (HU) changes, which indicate ventilation ability, are used as a weight for dose analysis. Therefore, we analyzed patients who had completed radiotherapy at the radiation oncology center of our hospital using 4DCT-ventilation imaging to determine the weight for a weighted-dose in order to explore the feasibility of the weighted-dose analysis for predicting RIP.

Materials and Methods

A total of 16 patients were included for analysis in the present study. The patient population consisted of 12 men and 4 women, aged between 46 and 66 years, with a median age of 56. Patients with squamous cell carcinoma (n = 6), adenocarcinoma (n = 6), and small-cell lung cancer (n = 4) received platinum-based double-drug chemotherapy with radiotherapy.

A 24-slice CT scanner (Siemens, Munich, Germany) was used to acquire 4-D data using an abdominal pressure respiratory induction system. The patients were placed in a supine position with their hands above their head, and were held in place by a thermoplastic reticular membrane during scanning.

The respiratory cycle was divided into 10 phases for data collection.¹⁴ A CT sequence was imaged with the patient breathing freely. The anatomy was scanned from the clavicle to the liver. Each patient's CT scan was reconstructed with a 3.0 mm slice thickness and transferred to the Pinnacle TPS 9.10.

All 16 patients were treated with a Trilogy linear accelerator (Varian Medical Systems, CA, USA) using a 6 MV photon beam. Intensity-modulated radiotherapy (IMRT) plans (named original plans, OPs) with 5-6 fields were designed for every patient, based on direct machine parameter optimization.

An OPs was designed for each of the 16 patients by the radiation oncology physicists once the internal target volume (ITV), planning target volume (PTV), and organs at risk (OAR) were defined by the doctors. The initial objective functions for the OPs are as follows: PTV – 60-66 Gy/30F, $D_{95\%} > 60-66$ Gy; heart – $V_{30} < 40\%$, $V_{40} < 30\%$; right lung and left lung – $V_5 < 65\%$, $V_{20} < 30\%$; esophagus – $V_{50} < 30\%$, $V_{60} < 10\%$; spinal cord – maximum dose (MaxD) < 45 Gy. These initial objective functions were used during the optimization, during which the physicists modified the objective functions several times until individualized optimal objective functions for each patient were established. The OPs were designed using free-breathing CT imaging because similar dosimetric characteristics between the free-breathing and the average intensity projection CTs have been reported in previous literature.^{15,16} Moreover, we had been using the free-breathing CT as the basis of planning, and were quite sure that it was better for the OP design. The left and right lungs were then merged into the A-Lung for evaluation. (**Note:** $D_{95\%}$ – minimum absorbed dose which reaches 95% of the target volume; V_x is the ratio between the volume of organs with absorbed a dose greater than x Gy and the total volume of organs)

A deformable image registration algorithm in MIM, (a software for imaging analysis, was used to register end-inhale CT sequences with the corresponding end-exhale CT sequences, in order to calculate a 4DCT-ventilation weighted-dose map for each patient.

In the present study, the end-inhale and end-exhale CT sequences were selected for the calculation of 4DCT-ventilation with a grid of 4.0 mm. The registration was used to calculate ventilation based on the HU density change, as follows¹⁰:

$$\frac{V_{in} - V_{ex}}{V_{ex}} = 1000 \frac{HU_{in} - HU_{ex}}{HU_{ex}(1000 + HU_{in})} \quad (1)$$

where V_{in} and V_{ex} are the end-inhale and end-exhale volumes, and HU_{in} and HU_{ex} are the end-inhale and end-exhale Hounsfield units of the individual lung voxels, respectively. HUs were defined as the average value in the 4.0 mm-grid, as this size grid is sufficient for the dose calculation of conventional fraction radiotherapy. During CT image reconstruction for planning, with a slice thickness of 3.0 mm, the grid would be slightly larger than 3.0 mm when calculating the average HU and 4DCT-ventilation.



Figure 1. The end-inhale computed tomography (CT) sequence was set as the “Planning CT (fixed image)”, shown in the first layer. The end-exhale CT sequence was set as the “Diagnostic CT (floating image)”, shown in the second layer. The Hounsfield unit (HU) density-change map was achieved using deformable image registration and was subtracted, as shown in the third layer.

Assuming that the original dose (OD) in the OP was $D_{0,i}$ and the weighted dose (WD) in the WP was $D_{w,i}$, the equation relating $D_{0,i}$ and $D_{w,i}$ was as follows:

$$D_{w,i} = D_{0,i} \left(1 + 1000 \frac{HU_{in,i} - HU_{ex,i}}{HU_{ex,i}(1000 + H_{in,i})} \right) \quad (2)$$

which considers the change in lung function identified by ventilation in each grid to calculate the dose.

The end-inhale and the end-exhale CT sequence images were subtracted to achieve $HU_{in,i} - HU_{ex,i}$ after registration, which created a ventilation map (VP) in A-Lung, as shown in Figure 1. Then, the VP and free-breathing CT underwent deformable image registration. The one-to-one correspondence between $D_{0,i}$ and $HU_{in,i} - HU_{ex,i}$ was used to calculate $D_{w,i}$, as shown in Figure 2.

The occurrence of radiation-induced pneumonia is related to many factors, and it is of great clinical significance to control these factors. Studies have shown that the dose factors heavily associated with radiation-induced pneumonia are V_5 , V_{20} , where $\Delta V_x = V_{w,x}$ in the WP - $V_{0,x}$ in the OP, and mean lung dose (MLD) calculated from A-Lung.¹⁷⁻¹⁹ Therefore, the parameters evaluated in the present study include V_5 , V_{20} , and MLD. The corresponding values after weighted-dose

calculation are $V_{5,w}$, $V_{20,w}$, and MLD_w , and their differences are ΔV_{20} ($V_{20,w} - V_{20}$), ΔV_5 ($V_{5,w} - V_5$), and ΔMLD ($MLD_w - MLD$). The correlations between the differences, ΔV_5 , ΔV_{20} , and ΔMLD , and the occurrence of radiation-induced pneumonia were analyzed.

Results

The average A-Lung values for V_5 , V_{20} , and MLD of the 16 patients were $67.9 \pm 7.5\%$ (55.4-80.2%), $29.9 \pm 2.9\%$ (26.3-38.6%), and 1741 ± 152 cGy (1504-2172 cGy) in the Ops, versus $79.2 \pm 6.8\%$ (67.3-88.6%), $38.4 \pm 2.7\%$ (34.7-44.2%), and 1916 ± 147 cGy (1645-2290 cGy) in the WPs, respectively, as shown in Table 1.

Based on the clinical symptoms of adverse events (RIP) described in the Common Terminology Criteria for Adverse Events 4.0 (CTCAE4.0), 3 radiation oncologists on the same team assessed and graded RIP. As shown in Table 2, 5 of the 16 patients had acute RIP (pneumonia which occurred < 1 month after the completion of radiotherapy), 4 of which (patients 3, 8, 11, and 15) had grade III RIP (patient required oxygen) and higher ΔV_5 , ΔV_{20} , and ΔMLD values compared to those of the other 12 patients, as shown in Table 1. However, the V_5 , V_{20} , and MLD values for those 4 patients were not at

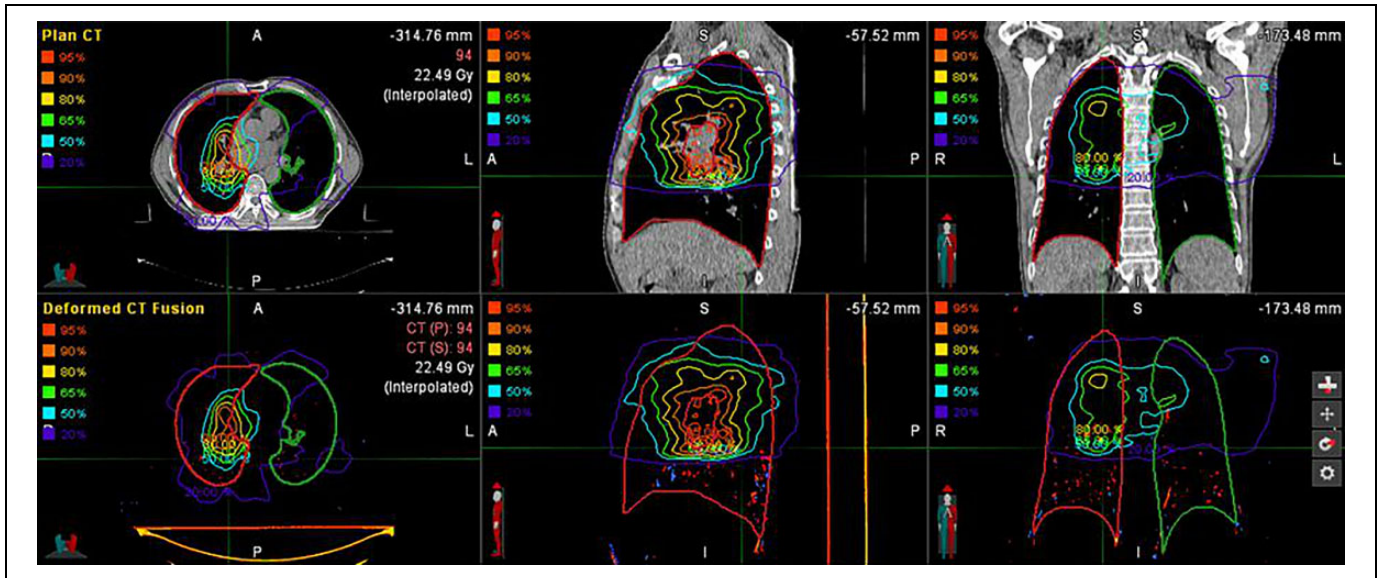


Figure 2. Deformable image registration of the free-breathing CT, which was the original plan (OP) design, and the HU density change map. The established one-to-one correspondence between $D_{0,i}$ and $HU_{in,i} - HU_{ex,i}$ was used for calculating $D_{w,i}$.

Table 1. Data Regarding the Original Dose (OD) in the Lung From the Original Plan (OP), the Weighted-Dose (WD) From the Weighted Plan (WP), and the Dose Difference (ΔD).^a

Pat.	$V_5(\%)$	$V_{20}(\%)$	MLD (cGy)	$V_{5,w}(\%)$	$V_{20,w}(\%)$	MLD _w (cGy)	$\Delta V_5(\%)$	$\Delta V_{20}(\%)$	ΔMLD (cGy)
1	80.2	30.2	1710	88.6	35.5	1854	8.4	5.3	144
2	59.3	31.4	1782	73.3	37.2	1931	14	5.8	149
3	55.4	26.6	1593	67.3	37.2	1889	11.9	10.6	296
4	78.6	38.6	2172	87.3	44.2	2290	8.7	5.6	118
5	62.2	28.2	1819	70.6	38.7	2025	8.4	10.5	206
6	73.1	31.9	1790	81.9	41.9	1911	8.8	10.0	121
7	68.5	27.7	1691	84.5	35.6	1843	16.0	7.9	152
8	65.7	28.5	1630	78.7	40.2	1863	13.0	11.7	233
9	74.3	32.2	1942	87.4	39.4	2132	13.1	7.2	190
10	72.4	31.3	1785	83.1	39.6	1953	10.7	8.3	168
11	68.5	30.0	1760	81.4	42.6	2018	12.9	12.6	258
12	67.2	26.3	1620	78.8	34.7	1751	11.6	8.4	131
13	77.5	30.9	1776	86.4	37.1	1886	8.9	6.2	110
14	65.8	30.2	1504	76.3	36.4	1645	10.5	6.2	141
15	56.5	27.7	1622	69.5	39.1	1890	13.0	11.4	268
16	61.5	27.3	1655	71.9	35.4	1778	10.4	8.1	123
Mean	67.9	29.9	1741	79.2	38.4	1916			
s	7.5	2.9	152	6.8	2.7	147			

^a ΔV_{20} ($V_{20,w} - V_{20}$), ΔV_5 ($V_{5,w} - V_5$), ΔMLD ($MLD_w - MLD$).

Table 2. Pneumonia Statistics Table.^a

Patient	1	2	3	4	5	6	7	8	9	10	11	12	13	14	15	16
Pneumonia		√	√					√			√				√	

^a“√” labels patients suffering from pneumonia.

the top of the OPs. The Spearman correlation analysis was used to analyze the correlation between RIP and ΔV_{20} , ΔMLD , and ΔV_5 . The results were as follows: RIP vs. ΔV_{20} , $r = 0.5123$; RIP vs. ΔMLD , $r = 0.5119$; and RIP vs. ΔV_5 , $r = 0.1904$.

Discussion

RIP is one of the major limitations of radiotherapy for patients with lung cancer. It is irreversible and may interrupt treatment, while at the same time, serious pneumonia may endanger the patient's life. RIP is influenced by a variety of factors.^{20,21} As of yet, the mechanisms of RIP are not well understood. The widely-accepted view at this time is that RIP is caused by damaged type II epithelial and endothelial cells and a series of signals from numerous acute inflammatory cells in locally damaged lungs.^{22,23} Irrespective of the pneumonia

pathogenesis, one important clinical phenomenon is the decline in ventilatory function once radiation-induced pneumonia occurs.²⁴

As functional imaging was lacking in the past, radiation oncologists held the opinion that the lung was a typical parallel organ, and that the function of each part was homogeneous, as was the radiation sensitivity. Thus, dose assessment usually focuses on the V_x and MLD of the entire lung, although dose location has not yet garnered much attention. Although there have been studies conducted based on the division of the lung into upper and lower parts, these results were rarely used in clinical practice.²⁵

After the development of functional imaging, lung function could be clearly evaluated, and the lung could be divided into the HFA and LFA, corresponding to good and poor ventilation, respectively. The information regarding HFAs and LFAs provided by lung-function imaging was used to make the therapeutic dose as small as possible in the HFA and protect the HFA in the design of the radiotherapy plan. The occurrence rate and severity of RIP are expected to be reduced by this method.²⁶⁻²⁸ However, one thing that was not demonstrated was the acquisition of HFA avoidance rather than loss of LFA involvement. This is very important, because no matter how the plans were designed, it was impossible to avoid HFAs completely, especially in cases with tumors located in HFAs. It is of note, however, that even in the HFA and LFA, lung function was not homogenous.

In the present study, we did not set any certain parameter by which to distinguish lung tissue into HFA and LFA, based on this knowledge. The function of each voxel/grid was labeled with 4DCT-ventilation, in an attempt to have the “label” reflect the dose of the voxel/grid. The results indicated that this method might be useful. Of the 16 patients, 5 patients (patients 3, 4, 8, 11, and 15) suffered from RIP. We considered V_5 , V_{20} , and MLD to be closely associated with RIP, and found that the V_5 of the OPs in patients 3, 4, 8, 11, and 15 ranked (from high to low) 16th, 2nd, 10th, 8th, and 15th, of 16 patients, V_{20} ranked 15th, 1st, 10th, 9th, and 13th, and MLD ranked 15th, 1st, 14th, 8th, and 13th. In other words, these patients did not rank in the top in for V_5 , V_{20} , or MLD; however, they suffered from RIP, while the other 11 patients with higher V_5 , V_{20} , and MLD values did not.

When $V_{5, w}$, $V_{20, w}$, and MLD_w were evaluated, it was easy to find that the ranking of ΔV_5 , ΔV_{20} , and ΔMLD for patients 3, 4, 8, 11, and 15 were at the top, particularly the ΔV_{20} and ΔMLD for patients 3, 8, 11, and 15. For patients 3, 8, 11, and 15, the rate of high-dose radiation exposure to the HFA was higher than that of the other patients. Subsequently, the HFA of the lung was more seriously damaged, which undoubtedly increased the probability of developing RIP. The results of the Spearman correlation analysis corroborated this, as for RIP vs. ΔV_{20} , $r = 0.5123$; RIP vs. ΔMLD , $r = 0.5119$; and RIP vs. ΔV_5 , $r = 0.1904$. Spearman’s rank-order correlation is a method used to study the correlation between 2 variables according to ranking data. The RIP correlation coefficients for

ΔV_{20} and ΔMLD were greater than 0.5, indicating a certain correlation between RIP and both ΔV_{20} and ΔMLD .

Of course, there were individual differences in the realized clinical probability. It was evident that of the 16 patients, the ΔV_{20} and ΔMLD for patient 5 were higher, however, the patient didn’t suffer from acute RIP.

There were many points worth discussing, if the weighted method was used to explain the clinical results of these 16 patients, such as how equation (2) expressed the weighted dose. By comparing equations (1) and (2), we found that equation (2) reflected the amount of air exchange in the grid (4.0 mm × 4.0 mm × 4.0 mm). The results of the present study showed that radiation sensitivity was positively correlated with oxygen amount, regardless of cells and tissues.²⁹⁻³² The ΔV_{20} and ΔMLD values found in the present study were produced by equation (2). Namely, the ΔV_{20} and ΔMLD were clinical (macro) manifestations of “oxygen concentration-increasing-radiosensitivity.”

However, the number of patients in the present study was small, and further studies are needed to evaluate whether this approach would have the same results in a larger sample. Additionally, there may be other factors that could have induced errors in the analysis, such as the CT used in the studies, artifacts, and ventilation reconstruction algorithms, which depend on the improvement of image processing technology and algorithms.

Conclusion

The 4DCT-ventilation-based weighted-dose analysis in the present study showed that there was some correlation between RIPP and both ΔV_{20} and ΔMLD , when comparing the weighted-dose and conventional DVH analyses.

Acknowledgements

We would like to thank Professor Jing Cai, Head of the Department of Medical Physics, The Hong Kong Polytechnic University for his guidance.

Author Contributions

Bai, Xia, and Li all contributed equally to the present study and share primary authorship.

Declaration of Conflicting Interests

The author(s) declared no potential conflicts of interest with respect to the research, authorship, and/or publication of this article.

Funding

The author(s) disclosed receipt of the following financial support for the research, authorship, and/or publication of this article: This work was supported by the National Key R&D Program of China (No.2018YFC1311400/2018YFC1311402) and by the Scientific and Public Welfare Project of the Tumor Precise Radiotherapy Spark Program (No.2019-N-11-29).

ORCID iD

Han Bai  <https://orcid.org/0000-0003-3593-1262>

References

1. Shaverdian N, Wang PC, Steinberg M, Lee P. The patient's perspective on stereotactic body radiation therapy (SBRT) vs. surgery for treatment of early stage non-small cell lung cancer (NSCLC). *Lung Cancer*. 2015;90(2):230-233. doi:10.1016/j.lungcan.2015.07.009
2. Onishi H, Shirato H, Nagata Y, et al. Stereotactic body radiotherapy (SBRT) for operable stage I non-small-cell lung cancer: can SBRT be comparable to surgery? *Int J Radiat Oncol Biol Phys*. 2011;81(5):1352-1358. doi:10.1016/j.ijrobp.2009.07.1751
3. Tian J, Luo Y, Xiang J, Tang J. Combined treatment for non-small cell lung cancer and breast cancer patients with brain metastases with whole brain radiotherapy and temozolomide: a systematic review and meta-analysis. *J Neurooncol*. 2017;135(2):217-227. doi:10.1007/s11060-017-2572-z
4. Marks LB, Bentzen SM, Deasy JO, et al. Radiation dose-volume effects in the lung. *Int J Radiat Oncol Biol Phys*. 2010;76(3 Suppl):S70-76. doi:10.1016/j.ijrobp.2009.06.091
5. St-Hilaire J, Lavoie C, Dagnault A, et al. Functional avoidance of lung in plan optimization with an aperture-based inverse planning system. *Radiother Oncol*. 2011;100(3):390-395. doi:10.1016/j.radonc.2011.09.003
6. Siva S, Thomas R, Callahan J, et al. High-resolution pulmonary ventilation and perfusion PET/CT allows for functionally adapted intensity modulated radiotherapy in lung cancer. *Radiother Oncol*. 2015;115(2):157-162. doi:10.1016/j.radonc.2015.04.013
7. Siva S, Devereux T, Ball DL, et al. Ga-68 MAA perfusion 4D-PET/CT scanning allows for functional lung avoidance using conformal radiation therapy planning. *Technol Cancer Res Treat*. 2016;15(1):114-121. doi:10.1177/1533034614565534
8. Lavrenkov K, Christian JA, Partridge M, et al. A potential to reduce pulmonary toxicity: the use of perfusion SPECT with IMRT for functional lung avoidance in radiotherapy of non-small cell lung cancer. *Radiother Oncol*. 2007;83(2):156-162. doi:10.1016/j.radonc.2007.04.005
9. Ireland RH, Bragg CM, McJury M, et al. Feasibility of image registration and intensity-modulated radiotherapy planning with hyperpolarized helium-3 magnetic resonance imaging for non-small-cell lung cancer. *Int J Radiat Oncol Biol Phys*. 2007;68(1):273-281. doi:10.1016/j.ijrobp.2006.12.068
10. Waxweiler T, Schubert L, Diot Q, et al. A complete 4DCT-ventilation functional avoidance virtual trial: developing strategies for prospective clinical trials. *J Appl Clin Med Phys*. 2017;18(3):144-152. doi:10.1002/acm2.12086
11. Vinogradskiy Y, Rusthoven CG, Schubert L, et al. Interim analysis of a two-institution, prospective clinical trial of 4DCT-ventilation-based functional avoidance radiation therapy. *Int J Radiat Oncol Biol Phys*. 2018;102(4):1357-1365. doi:10.1016/j.ijrobp.2018.07.186
12. Vinogradskiy Y, Schubert L, Diot Q, et al. Regional lung function profiles of stage I and III lung cancer patients: an evaluation for functional avoidance radiation therapy. *Int J Radiat Oncol Biol Phys*. 2016;95(4):1273-1280. doi:10.1016/j.ijrobp.2016.02.058
13. Wang R, Zhang S, Yu H, et al. Beam orientation optimization of pulmonary ventilation image-guided intensity modulated radiotherapy for lung cancer. *Clin J Radiol Med Prot*. 2015;35(3):201-205. doi:10.3760/cma.j.issn.0254-5098
14. Rasheed A, Jabbour SK, Rosenberg S, et al. Motion and volumetric change as demonstrated by 4DCT: the effects of abdominal compression on the GTV, lungs, and heart in lung cancer patients. *Pract Radiat Oncol*. 2016;6(5):352-359. doi:10.1016/j.prro.2015.12.006
15. Tian Y, Wang Z, Ge H, et al. Dosimetric comparison of treatment plans based on free breathing, maximum, and average intensity projection CTs for lung cancer SBRT. *Med Phys*. 2012;39(5):2754-2760. doi:10.1118/1.4705353
16. Han K, Basran PS, Cheung P. Comparison of helical and average computed tomography for stereotactic body radiation treatment planning and normal tissue contouring in lung cancer. *Clin Oncol*. 2010;22(10):862-867. doi:10.1016/j.clon.2010.08.010
17. Deek MP, Nagarajan S, Kim S, et al. Clinical characteristics and dose-volume histogram parameters associated with the development of pleural effusions in non-small cell lung cancer patients treated with chemoradiation therapy. *Acta Oncol*. 2016;55(8):1029-1035. doi:10.1080/0284186X.2016.1176248
18. Takahashi S, Go T, Kasai Y, Yokomise H, Shibata T. Relationship between dose-volume parameters and pulmonary complications after neoadjuvant chemoradiotherapy followed by surgery for lung cancer. *Strahlenther Onkol*. 2016;192(9):658-667. doi:10.1007/s00066-016-1021-9
19. Ogata T, Katsui K, Yoshio K, et al. Dose-volume parameters predict radiation pneumonitis after surgery with induction concurrent chemoradiotherapy for non-small cell lung cancer. *Acta Med Okayama*. 2018;72(5):507-513. doi:10.18926/AMO/56249
20. Ogata K, Kawarada Y, Shibata K, Nishio T, Hara N. Pulmonary radiation injury manifested by signs of bronchiolitis obliterans with organizing pneumonia after postoperative breast cancer radiotherapy. *Nihon Kokyuki Gakkai Zasshi*. 1999;37(12):979-982.
21. Solomon J, Schwarz M. Drug-, toxin-, and radiation therapy-induced eosinophilic pneumonia. *Semin Respir Crit Care Med*. 2006;27(2):192-197. doi:10.1055/s-2006-939522
22. Yoneshige A, Hagiyaama M, Inoue T, et al. Increased ectodomain shedding of cell adhesion molecule 1 as a cause of type II alveolar epithelial cell apoptosis in patients with idiopathic interstitial pneumonia. *Respir Res*. 2015;16:90. Published 2015 Aug 1. doi:10.1186/s12931-015-0255-x
23. Waisberg DR, Barbas-Filho JV, Parra ER, et al. Abnormal expression of telomerase/apoptosis limits type II alveolar epithelial cell replication in the early remodeling of usual interstitial pneumonia/idiopathic pulmonary fibrosis. *Hum Pathol*. 2010;41(3):385-391. doi:10.1016/j.humpath.2009.08.019
24. Vinogradskiy Y, Faught A, Castillo R, et al. Using 4DCT-ventilation to characterize lung function changes for pediatric patients getting thoracic radiotherapy. *J Appl Clin Med Phys*. 2018;19(5):407-412. doi:10.1002/acm2.12397
25. Deasy JO, EI Naqa I. Image-based modeling of normal tissue complication probability for radiation therapy. *Cancer Treat Res*. 2008;139:215-256.
26. Vinogradskiy Y, Castillo R, Castillo E, et al. Use of 4-dimensional computed tomography-based ventilation imaging

- to correlate lung dose and function with clinical outcomes. *Int J Radiat Oncol Biol Phys*. 2013;86(2):366-371. doi:10.1016/j.ijrobp.2013.01.004
27. Kadoya N, Cho SY, Kanai T, et al. Dosimetric impact of 4-dimensional computed tomography ventilation imaging-based functional treatment planning for stereotactic body radiation therapy with 3-dimensional conformal radiation therapy. *Pract Radiat Oncol*. 2015;5(5):e505-e512. doi:10.1016/j.pro.2015.03.001
28. Sharifi H, Brown S, McDonald GC, Chetty IJ, Zhong H. 4-Dimensional computed tomography-based ventilation and compliance images for quantification of radiation-induced changes in pulmonary function. *J Med Imaging Radiat Oncol*. 2019;30(1):560-565. doi:10.1111/1754-9485.12881
29. Potten CS, Howard A. Radiation depigmentation of mouse hair: the influence of local tissue oxygen tension on radiosensitivity. *Radiat Res*. 1969;38(1):65-81.
30. Jamieson D, Vandenbrenk HA. Effect of progressive changes in body temperature of rats on tissue oxygen-tensions, in relation to radiosensitivity. *Int J Radiat Biol Relat Stud Phys Chem Med*. 1963;6:529-540. doi:10.1080/09553006314550641
31. Dewey DL. Effect of oxygen and nitric oxide on the radiosensitivity of human cells in tissue culture. *Nature*. 1960;186:780-782. doi:10.1038/186780a0
32. Hewitt HB, Wilson CW. The effect of tissue oxygen tension on the radiosensitivity of leukaemia cells irradiated in situ in the livers of leukaemic mice. *Br J Cancer*. 1959;13(4):675-684. doi:10.1038/bjc.1959.75